Corrole Chemistry

International Edition: DOI: 10.1002/anie.201508829
German Edition: DOI: 10.1002/ange.201508829

Bipyricorrole: A Corrole Homologue with a Monoanionic Core as a Fluorescence Zn^{II} Sensor

*B. Adinarayana, Ajesh P. Thomas, Prerna Yadav, Arun Kumar, and A. Srinivasan**

Dedicated to Professor Vadapalli Chandrasekhar

Abstract: *In the corrole homologue, 6,11,16-triarylbipyricorrole, the bipyrrole unit is replaced by a 2,2′-bipyridine unit. This modification effectively alters the corrole N4 coordination sphere from the trianionic $[(NH)_3N]$ to the monoanionic $[N_3NH]$ state. The newly formed monoanionic core stabilizes Zn^{II} ions with enhanced emission properties. The enhanced emission was further utilized for metal ion sensing studies and exploited for the selective detection of Zn^{II} ions.*

Corroles (**1**) are contracted porphyrinoids with 2,2′-bipyrrole units in the macrocyclic framework, and thus constitute a bridge between corrin and porphyrin units (Figure 1).[1] The

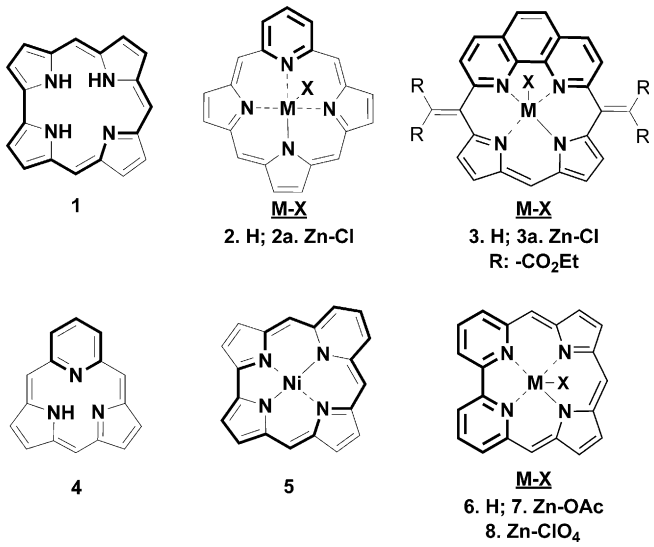

Figure 1. Structures of porphyrin and contracted homologues.

trianionic core is known to stabilize higher oxidation state metal complexes, and are widely applied in catalysis, sensors, and dye-sensitized solar cells.[2] Structural modification in the framework alters the electronic structure, thereby leading to unusual optical, photophysical, and coordination properties.[3] A series of core-modified corroles, such as *iso*-carbacorrole,[3a] N-confused derivative,[3b] norrole,[3c] benzonorrole,[3d] oxacorrole,[3e,f] diaoxacorrole,[3g] and thiacorrole,[3h] were introduced. Recently, we reported a *meso*-aryl biphenylcorrole, where the bipyrrole moiety is replaced by biphenyl unit and the trianionic core stabilizes Cu^{III} ions.[4] In a continuation of our ongoing research, the next target in this series is to introduce a pyridyl/bipyridyl unit in the molecular framework and explore its properties.

The pyridine-based porphyrinoid, pyriporphyrinone, was reported by Berlin and Breitmaier, where the carbonyl group was inserted in the *meso*-position.[5a] Since then, several pyridyl derivatives have been reported, including pyriporphyrin (**2**) and its Zn^{II} (**2a**) and Fe^{III} complexes,[5b] confused pyriporphyrin[5c–f] and its Fe^{II}, Fe^{III},[5c–e] and Pd^{II} complexes,[5f] oxypyriporphyin[6a–d] and its Ni^{II}[6e] and Fe^{III}[6f] complexes, and a dipyridinoid-substituted porphyrin[6g] derivative. Similarly, a variety of pyridine-based derivatives have been described and characterized: (i) expanded porphyrins,[7] such as 12-hydroxypyrisapphyrin,[7a] dipyrihexaphyrin,[7b–d] tetrapyrioctaphyrin,[7e] bipyrioctaphyrin,[7f] and cyclo[*m*]pyridine-[*n*]pyrroles;[7g,h] (ii) phthalocyanine derivatives such as hemiporphyrazines;[8] (iii) calixpyrrole derivatives such as *meso*-octaethyl calix[4]pyridine;[9] and (iv) cryptand-like pyriporphyrinoid macrocycles.[10] Recently, a series of porphyrin-related macrocycles with N4 coordination spheres were reported, including: 1,10-phenanthroline-embedded porphyrins (**3**) as Mg^{II} sensors;[11] carbazole and pyridine building blocks with high-spin Co^{II} complexes;[12a] and cobalt(II) phenanthroline-indole macrocycles as electrocatalysts for oxygen reduction.[12b] However, the pyridine-based contracted porphyrinoids are scarcely reported. The subpyriporphyrin (**4**) was synthesized by Latos–Grażyński and co-workers, who described its reaction with a boron complex.[13] Recently, the nickel(II) pyricorrole (**5**) was reported by Neya and co-workers.[14] Overall, the corrole and its modified derivatives are in the di- or trianionic form in the neutral state. The monoanionic form,[3g] however, is scarcely reported. It is important to note that the basic framework of biologically important cob(I)alamin is constituted by corrin units, which are in the monoanionic state and stabilize the Co^{III} ion.[15] Herein, we report the synthesis of monoanionic corrole, 6,11,16-triarylbipyricorrole (**6**), and its Zn^{II} complex (**7** and **8**). Introduction of a 2,2′-bipyridyl unit in the macrocycle is unprecedented in the corrole chemistry and provides a stable tetra-nitrogen (NNNN) core with monoanionic charge. The zinc complex is stabilized by the monoanionic core with axial coordination, and exhibits Chelation-Induced Emission Enhancement (CIEE)[16] upon metal ion insertion.

[*] B. Adinarayana, Dr. A. P. Thomas, P. Yadav, Dr. A. Kumar, Dr. A. Srinivasan
School of Chemical Sciences
National Institute of Science Education and Research (NISER)
Bhubaneswar - 751005, Odisha (India)
E-mail: srini@niser.ac.in

Supporting information for this article is available on the WWW under http://dx.doi.org/10.1002/anie.201508829.

The synthesis of compound **6** and its coordination chemistry is described in Scheme 1. The target macrocycle was achieved in four steps. The first step was the synthesis of 2,2′-bipyridine-6,6′-diylbis(phenylmethanone) (**10**) from 2,2′-bipyridine-6,6′-dicarbonitrile (**9**)[17] by using freshly prepared phenylmagnesium bromide in THF in 75% yield. Sodium

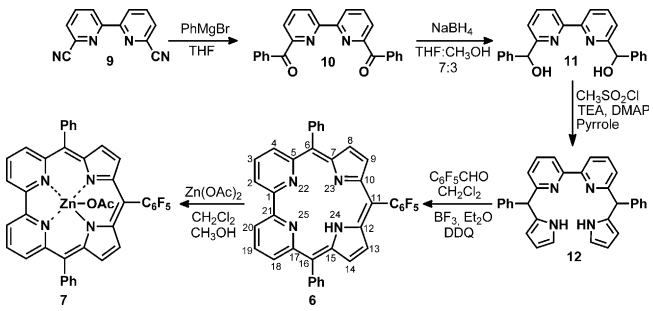

Scheme 1. Synthesis of **6** and **7**.

borohydride reduction of **10** in THF:CH_3OH (7:3) formed 6,6′-bis(phenylhydroxymethyl)-2,2′-bipyridine (**11**) in quantitative yield in the second step. The key precursor (**12**) was synthesized in the third step, where the direct conversion of **11** in the presence of excess pyrrole and $BF_3{\cdot}Et_2O$ as an acid catalyst was not successful. Instead, we adopted a strategy as similar to that reported by Latos–Grażyński,[5b,c] where compound **11** was reacted with methanesulphonyl chloride, TEA, and DMAP, followed by condensation with 100 equiv of pyrrole, afforded **12** in 40% yield. The target macrocycle was achieved in the final step by an acid-catalyzed condensation reaction of **12** with pentafluorobenzaldehyde in the presence of trifluoroacetic acid (TFA) in CH_2Cl_2, followed by oxidation with 2,3-dichloro-5,6-dicyano-*p*-benzoquinone (DDQ). The crude mixture was purified by column chromatographic separation, where a blue color fraction, eluted with CH_2Cl_2 and CH_3OH (99:1), was identified as **6** in 12% yield. The coordination chemistry of **6** was further examined by using $Zn(OAc)_2$ in CH_2Cl_2/CH_3OH mixture, where the green fraction was eluted from a silica gel column, to afford **7** in quantitative yield. The ESI-Q-TOF analysis showed the molecular ion signals of **6** and Zn^{II} complex (**7**) at *m*/*z* 641.1664 [$M+1$] and 703.0741 [*M*-OAc], and confirmed the exact composition.

The ^1H NMR spectrum of **6** and **7** was recorded in $CDCl_3$ at 298 K. The bipyridyl protons in **6** were detected as two doublets at 8.16 [H4 and H18] and 7.36 [H2, H20] ppm, and a triplet at 7.87 [H3, H19] ppm. The pyrrolic β-CH protons appeared as a doublet at 6.91 [H8, H14] and 6.46 [H9, H13] ppm, respectively. The pyrrolic NH [H24] is observed as a broad singlet at 11.77 ppm, which was further confirmed by a $CDCl_3/D_2O$ exchange experiment. The *meso*-phenyl protons appeared at 7.50 ppm. Overall, the peak positions of **6** are consistent with nonaromatic character.[4,11a] On the other hand, the absence of an inner NH signal, and slightly deshielded bipyridyl, pyrrolic β-CH protons confirm the metal ion insertion in **6** to form **7**. The bipyridyl protons in **7** were observed at 8.81 [H4, H18], 8.33 [H3, H19], and 8.02 [H2, H20] ppm, while the pyrrolic β-CH protons were observed at 7.16 [H8, H14] and 6.87 [H9, H13] ppm. These signals were further confirmed by 2D homonuclear correlation spectroscopy (Supporting Information, Figure S18). The *meso*-phenyl protons appeared at 7.58 ppm. Furthermore, the singlet peak at 1.62 ppm was assigned to the methyl group from the axially coordinated acetate ion, suggesting that the Zn^{II} ion is stabilized by the monoanionic core.

The structures of **6** and **7** were confirmed by single-crystal X-ray analysis (Figure 2; Supporting Information, Table S5).

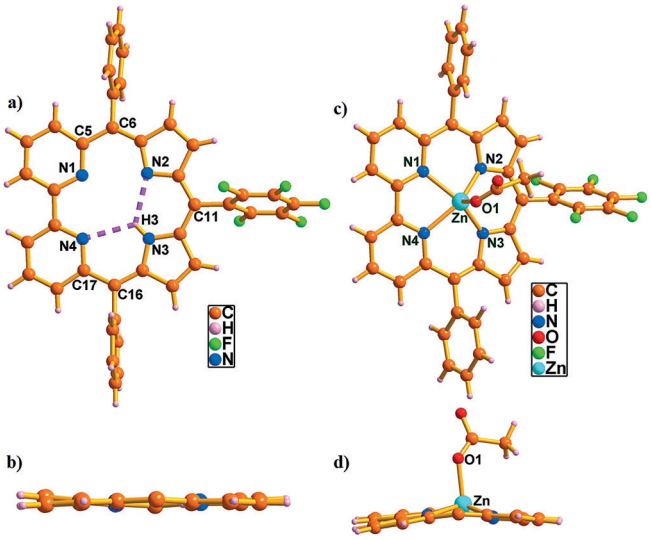

Figure 2. Single-crystal X-ray structures of **6** and **7**. Top view (a, c) and side view (b, d). The *meso*-aryl groups are omitted for clarity in the side view.

As predicted from the spectral analysis, the nonaromatic character in **6** is further reflected from the crystal analysis, where i) the bipyridyl unit and dipyrromethene moieties are connected by sp^2-sp^2 single bond character, with the bond lengths of 1.455 Å (C5–C6) and 1.472 Å (C16–C17); ii) the sp^2-sp^2 double bond character (bond lengths between 1.337 and 1.399 Å), and the average bond angle (119.996°) within the bipyridyl unit[18] maintains the individual aromatic character; and iii) the sp^2-sp^2 single and double bond character (bond lengths between 1.336 and 1.472 Å) within the dipyrromethene moiety support the effective π-delocalization (Figure S30, Table S1). Thus, the individual aromaticity in the bipyridyl unit and the π-conjugation within the dipyrromethene moiety remain isolated from the overall macrocyclic aromatization. Furthermore, the saddling dihedral angles (χ_1–χ_4) are between 3.90° and 7.35° (Table S4), which are far less than those found in **1** and its derivatives.[19a] The pyrrole units are hardly deviated from the mean N4 plane, with a maximum deviation of 5.913°, suggesting that the macrocycle **6** adopts planar conformation (Figure 2b). The amine hydrogen (N3-H3) in the pyrrolic unit is engaged in intramolecular hydrogen bonding with the neighboring imine nitrogens of pyrrole (N2), as well as the pyridine unit (N4). The bond lengths and angles of N3-H3··N2 and N3-H3··N4 are 2.23 Å and 122.31°, and 2.34 Å and 118.27°, respectively (Figure 2a).

Metal ion insertion and axial coordination is also reflected in the single crystal X-ray structure of **7** (Figure 2c), where the Zn^{II} ion is 0.54 Å above the mean N4 plane (Figure 2d). The geometry around the metal center is square pyramid, with four nitrogens in the equatorial plane and the fifth position occupied by an axially coordinated acetate ion. The bond lengths of Zn–N1 and Zn–N4 are 2.120 and 2.114 Å, which are longer than Zn–N2 and Zn–N3 with values of 2.016 and 1.997 Å, (Figure S31, Table S2). The bond lengths are comparable with **2a** [Zn-$N_{pyridine}$: 2.35 Å and Zn-$N_{pyrrole}$: 2.05–2.11 Å][5b] and **3a** [Zn-$N_{pyridine}$: 2.16–2.17 Å and Zn-$N_{pyrrole}$: 2.03–2.04 Å].[11b] Furthermore, the saddling dihedral angle values (χ_1–χ_4) in **7** are between 2.526° and 11.809°[19b] (Table S4); the pyrrole units are slightly tilted from the mean N4 plane, with a maximum deviation of 12.468°. The presence of fluorine atoms in the pentafluoro unit generates intermolecular hydrogen bonding interactions, where one of the *meso*-phenyl-CHs (C23–H23) interacts with the neighboring molecule fluorine atom (F3) to generate a hexameric structure in the solid state. The units are arranged in alternating fashion, where the distance between the adjacent, alternate, and the opposite Zn^{II} ions are 13.84 Å, 20.25 Å, and 24.53 Å, respectively, with the cavity size of 1563 $Å^3$ (Figure S26).

The electronic absorption and emission spectrum of both **6** and **7** in CH_3OH is shown in Figure 3, along with visible and

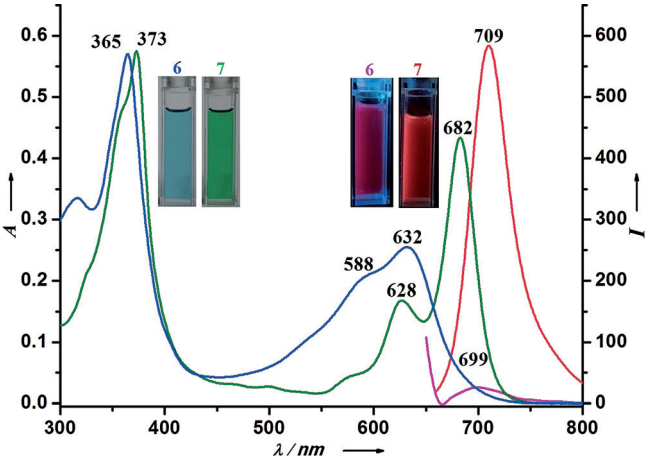

Figure 3. The electronic absorption and emission spectrum of **6** and **7** in CH_3OH along with absorption (left) and emission (right) color changes.

emission color changes. The absorption spectrum of **6** shows an intense band at 365 nm and the weak Q-type bands between 588 and 632 nm, respectively, with the molar extinction coefficient of 10^5. The spectral results of **6** were compared with biphenylcorrole,[4] **2**,[5b] and **1**,[2a] and the results are summarized as follows: i) the molar absorption coefficient and the spectral pattern are similar to biphenylcorrole[4] and **2**,[5b] reflecting the nonaromatic character in **6**; ii) the intense band and weak Q-bands in **6** are blue shifted by 46 and 53 nm, as compared to **2**,[5b] suggesting a reduction in the π-delocalization (dipyrromethene vs. tripyrromethene); and iii) the absence of the Soret band and a reduction in the molar absorption coefficient of the intense band as compared to **1**,[2a] indicating that **6** is not aromatic. Upon Zn^{II} ion insertion (**7**), the color of the solution changes from blue to green. The intense band and weak Q-bands in **6** are redshifted by 8 and 40–50 nm, and observed at 373 and 628–682 nm, respectively, with a moderate increase in the ε value. The results are further compared with **2a**,[5b] where the Q-band is 166 nm blue shifted, suggesting that **7** has less π-delocalization and maintains nonaromaticity.

The emission spectrum of **6** shows a weaker band at 699 nm with the fluorescence quantum yield (Φ_F) of 0.011. Upon chelation, the emission color changes from light brickred to intense red and the band is redshifted by 10 nm and appears at 709 nm with eight-fold increase in emission intensity and the quantum yield (Φ_F) is 0.089. It is pertinent to point out here that there is no emission intensity observed in the case of Zn^{II} complex of N-substituted derivative **1**[20] and **2a**.[5b] The Chelation-Induced Emission Enhancement (CIEE) character shown by **6** upon Zn^{II} metalation may find potential application in biological imaging.[21]

The enhanced emission upon Zn^{II} ion insertion prompted us to perform sensing studies of **6** to determine whether **6** is selective towards Zn^{II} ion or any other metal ions. A preliminary qualitative experiment was performed by using dilute CH_3OH solution of **6** with 10 equiv of various metal ions, such as Ag^{I}, Ca^{II}, Cd^{II}, Co^{II}, Cr^{III}, Cu^{II}, Fe^{III}, Hg^{II}, Mg^{II}, Mn^{II}, Ni^{II}, and Zn^{II}, in the form of perchlorate (ClO_4^-) salts. Among the tested metal ions, only the Zn^{II} ion exhibited turn-on emission (Figure 4a). To have a quantitative picture, various equivalents of Zn^{II} ions were gradually added to the 10 μM CH_3OH solution of **6**. Upon increasing the concentration of Zn^{II} ions, the intensity of the emission band increased gradually up to 1 equiv. Further increasing the

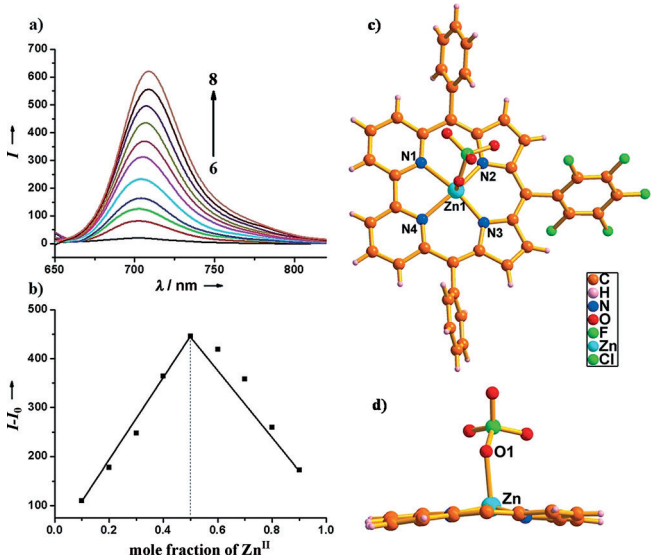

Figure 4. Sensing properties of **6**. a) The emission spectral changes upon addition of Zn^{II} in CH_3OH solution. b) The Job's plot for the complexation. c, d) Single-crystal X-ray structure of **8**. Top view (c) and side view (d). The *meso*-aryl groups are omitted for clarity in the side view.

concentration of Zn^{II} ion failed to produce an appreciable change in the emission intensity. The Job's plot showing the change in the emission spectral data suggests formation of 1:1 binding mode (Figure 4b), and the association constant is $5.47 \times 10^4\,M^{-1}$ from the Benesi–Hildebrand plot. The competitive recognition studies of the Zn^{II} ion over other metal ions found that **6** selectively senses Zn^{II} ions, even in the presence of 100 equiv of other ions (Figures S43–S44), and the detection limit was found to be 1.5 ppm. The experiments were also conducted in 0.1 M HEPES buffer (pH 7.4) aqueous/CH_3OH solution (CH_3OH/H_2O; 4:6 v/v), and similar trends were observed (Figures S39–S40).

The newly formed 1:1 complex (**8**) was further characterized by mass spectral analysis, and showed the molecular ion signal at *m*/*z* 703.0888 [*M*-ClO_4]. ^{1}H NMR analysis demonstrated that the complex retained nonaromatic character (Figures S19–S21). Finally, the complex was unambiguously confirmed by single-crystal X-ray analysis, where the geometry around the metal center was found to be square pyramid (Figure 4c; Supporting Information, Table S5). The Zn^{II} ion is 0.35 Å above the mean N4 plane and perchlorate ion is axially coordinated (Figure 4d). As observed in **7**, the $Zn{-}N_{pyridine}$ bond lengths in **8** are 2.11 to 2.12 Å, which are longer than the $Zn{-}N_{pyrrole}$ bond lengths with values of 1.98 and 2.02 Å, respectively (Figure S32, Table S3).

In summary, we have successfully synthesized 6,11,16-triarylbipyricorrole and its Zn^{II} complex. Their nonaromatic character was demonstrated by spectral studies and structural analysis. To the best of our knowledge, the monoanionic core stabilizes the Zn^{II} ion without altering the internal coordination sphere, which was previously unprecedented in corrole chemistry. The enhanced emission upon metal ion insertion was further exploited for sensing studies, where the ligand was effectively utilized for selective detection of Zn^{II} over other metal ions by retaining the nonaromaticity. The flexible axial coordination in **6** provides an advantage for the development of catalytic and biomimetic models, and efforts exploring this chemistry is currently the direction of our research group.

Acknowledgements

Dr. A.S. thanks NISER, Department of Atomic Energy for financial support. B.A. thanks CSIR for the fellowship.

Keywords: bipyridyl units · corroles · monoanionic · nonaromaticity · sensing studies

How to cite: *Angew. Chem. Int. Ed.* **2016**, *55*, 969–973
Angew. Chem. **2016**, *128*, 981–985

[1] a) R. Paolesse in *The porphyrin Handbook*, *Vol. 2* (Eds.: K. M. Kadish, K. M. Smith, R. Guilard), Academic Press, New York, **2000**, pp. 201–232; b) C. Erben, S. Will, K. M. Kadish in *The Porphyrin Handbook*, *Vol. 2* (Eds.: K. M. Kadish, K. M. Smith, R. Guilard), Academic Press, New York, **2000**, pp. 233–300.

[2] a) Z. Gross, N. Galili, I. Saltsman, *Angew. Chem. Int. Ed.* **1999**, *38*, 1427–1429; *Angew. Chem.* **1999**, *111*, 1530–1533; b) I. Aviv, Z. Gross, *Chem. Commun.* **2007**, 1987–1997; c) L. Flamigni, D. T. Gryko, *Chem. Soc. Rev.* **2009**, *38*, 1635–1646.

[3] a) J. Skonieczny, L. Latos-Grażyński, L. Szterenberg, *Chem. Eur. J.* **2008**, *14*, 4861–4874; b) K. Fujino, Y. Hirata, Y. Kawabe, T. Morimoto, A. Srinivasan, M. Toganoh, Y. Miseki, A. Kudo, H. Furuta, *Angew. Chem. Int. Ed.* **2011**, *50*, 6855–6859; *Angew. Chem.* **2011**, *123*, 6987–6991; c) M. Toganoh, Y. Kawabe, H. Furuta, *J. Org. Chem.* **2011**, *76*, 7618–7622; d) M. Toganoh, Y. Kawabe, H. Uno, H. Furuta, *Angew. Chem. Int. Ed.* **2012**, *51*, 8753–8756; *Angew. Chem.* **2012**, *124*, 8883–8886; e) B. Sridevi, S. J. Narayanan, T. K. Chandrashekar, U. Eglich, K. R-Senge, *Chem. Eur. J.* **2000**, *6*, 2554–2563; f) C.-H. Lee, W.-S. Cho, J.-H. Ka, P. H. Lee, *Bull. Korean Chem. Soc.* **2000**, *21*, 429–433; g) M. Pawlicki, L. Latos-Grażyński, L. Szterenberg, *J. Org. Chem.* **2002**, *67*, 5644–5653; h) V. S. Shetti, U. R. Prabhu, M. Ravikanth, *J. Org. Chem.* **2010**, *75*, 4172–4182.

[4] B. Adinarayana, A. P. Thomas, C. H. Suresh, A. Srinivasan, *Angew. Chem. Int. Ed.* **2015**, *54*, 10478–10482; *Angew. Chem.* **2015**, *127*, 10624–10628.

[5] a) K. Berlin, E. Breitmaier, *Angew. Chem. Int. Ed. Engl.* **1994**, *33*, 219–220; *Angew. Chem.* **1994**, *106*, 229–230; b) R. Myśliborski, L. Latos-Grażyński, L. Szterenberg, *Eur. J. Org. Chem.* **2006**, 3064–3068; c) R. Myśliborski, L. Latos-Grażyński, *Eur. J. Org. Chem.* **2005**, 5039–5048; d) R. Myśliborski, K. Rachlewicz, L. Latos-Grażyński, *Inorg. Chem.* **2006**, *45*, 7828–7834; e) R. Myśliborski, K. Rachlewicz, L. Latos-Grażyński, *J. Porphyrins Phthalocyanines* **2007**, *11*, 172–180; f) T. D. Lash, K. Pokharel, J. M. Serling, V. R. Yant, G. M. Ferrence, *Org. Lett.* **2007**, *9*, 2863–2866.

[6] a) T. D. Lash, S. T. Chaney, *Chem. Eur. J.* **1996**, *2*, 944–948; b) T. Schönemeier, E. Breitmaier, *Synthesis* **1997**, 273–275; c) T. D. Lash, S. T. Chaney, D. T. Richter, *J. Org. Chem.* **1998**, *63*, 9076–9088; d) D. Liu, G. M. Ferrence, T. D. Lash, *J. Org. Chem.* **2004**, *69*, 6079–6093; e) K. R. Adams, R. Bonnett, P. J. Burke, A. Salgado, M. A. Vallés, *J. Chem. Soc. Perkin Trans.* **1997**, *1*, 1769–1772; f) S. Neya, M. Suzuki, H. Ode, T. Hoshino, Y. Furutani, H. Kandori, H. Hori, K. Imai, T. Komatsu, *Inorg. Chem.* **2008**, *47*, 10771–10778; g) S. Neya, M. Suzuki, T. Mochizuki, T. Hoshino, A. T. Kawaguchi, *Eur. J. Org. Chem.* **2015**, 3824–3829.

[7] a) D. T. Richter, T. D. Lash, *J. Org. Chem.* **2004**, *69*, 8842–8850; b) R. J. P. Corriu, G. Bolin, J. J. E. Moreau, C. Vernhet, *J. Chem. Soc. Chem. Commun.* **1991**, 211–213; c) F. H. Carré, R. J. P. Corriu, G. Bolin, J. J. E. Moreau, C. Vernhet, *Organometallics* **1993**, *12*, 2478–2486; d) J.-I. Setsune, K. Yamato, *Chem. Commun.* **2012**, *48*, 4447–4449; e) T. W. Bell, P. J. Cragg, M. G. B. Drew, A. Firestone, A. D. I. Kwok, J. Liu, R. T. Ludwig, A. T. Papoulis, *Pure Appl. Chem.* **1993**, *65*, 361–366; f) J.-I. Setsune, M. Kawama, T. Nishinaka, *Tetrahedron Lett.* **2011**, *52*, 1773–1777; g) Z. Zhang, J. M. Lim, M. Ishida, V. V. Roznyatovskiy, V. M. Lynch, H.-Y. Gong, X. Yang, D. Kim, J. L. Sessler, *J. Am. Chem. Soc.* **2012**, *134*, 4076–4079; h) Z. Zhang, W.-Y. Cha, N. J. Williams, E. L. Rush, M. Ishida, V. M. Lynch, D. Kim, J. L. Sessler, *J. Am. Chem. Soc.* **2014**, *136*, 7591–7594.

[8] F. Fernández-Lázaro, T. Torres, B. Hauschel, M. Hanack, *Chem. Rev.* **1998**, *98*, 563–575.

[9] V. Král, P. A. Gale, P. Anzenbacher, Jr., K. Jursíková, V. Lynch, J. L. Sessler, *Chem. Commun.* **1998**, 9–10.

[10] J.-I. Setsune, K. Watanabe, *J. Am. Chem. Soc.* **2008**, *130*, 2404–2405.

[11] a) M. Ishida, Y. Naruta, F. Tani, *Angew. Chem. Int. Ed.* **2010**, *49*, 91–94; *Angew. Chem.* **2010**, *122*, 95–98; b) M. Ishida, J. M. Lim, B. S. Lee, F. Tani, J. L. Sessler, D. Kim, Y. Naruta, *Chem. Eur. J.* **2012**, *18*, 14329–14341.

[12] a) L. Arnold, H. Norouzi-Arasi, M. Wagner, V. Enkelmann, K. Müllen, *Chem. Commun.* **2011**, *47*, 970–972; b) M. Quernheim, H. Liang, Q. Su, M. Baumgarten, N. Koshino, H. Higashimura, K. Müllen, *Chem. Eur. J.* **2014**, *20*, 14178–14183.

[13] a) R. Myśliborski, L. Latos-Grażyński, L. Szterenberg, T. Lis, *Angew. Chem. Int. Ed.* **2006**, *45*, 3670 – 3674; *Angew. Chem.* **2006**, *118*, 3752 – 3756.

[14] S. Neya, M. Suzuki, T. Matsugae, T. Hoshino, *Inorg. Chem.* **2012**, *51*, 3891 – 3895.

[15] a) A. S. Rury, T. E. Wiley, R. J. Sension, *Acc. Chem. Res.* **2015**, *48*, 860 – 867; b) F. Zelder, *Chem. Commun.* **2015**, *51*, 14004 – 14017.

[16] Chelation Enhanced Fluorescence (CHEF) is the emission phenomenon commonly used in chelation studies. See: R. D. Hancock, *Chem. Soc. Rev.* **2013**, *42*, 1500 – 1524 and the references cited therein. The term AIE (Aggregation Induced Emission) and AIEE (Aggregation Induced Emission Enhancement) are two different emission phenomena widely used in aggregation studies. See: a) Y. Hong, J. W. Y. Lam, B. Z. Tang, *Chem. Soc. Rev.* **2011**, *40*, 5361 – 5388; b) B.-K. An, J. Gierschner, S. Y. Park, *Acc. Chem. Res.* **2012**, *45*, 544 – 554 and the references cited therein. Based on this, we have introduced the term Chelation-Induced Emission Enhancement(CIEE), where the weak emission property of **6** is further enhanced upon chelation.

[17] V-M. Mukkala, M. Kwiatkowski, J. Kankare, H. Takalo, *Helv. Chim. Acta* **1993**, *76*, 893 – 899.

[18] L. L. Merritt, Jr., E. D. Schroeder, *Acta Crystallogr.* **1956**, *9*, 801 – 804.

[19] a) J. Capar, J. Conradie, C. M. Beavers, A. Ghosh, *J. Phys. Chem. A* **2015**, *119*, 3452 – 3457; b) K. E. Thomas, A. B. Alemayehu, J. Conradie, C. M. Beavers, A. Ghosh, *Acc. Chem. Res.* **2012**, *45*, 1203 – 1214.

[20] a) R. Paolessee, S. Licoccia, T. Boschi, *Inorg. Chim. Acta* **1990**, *178*, 9 – 12; b) Z. Gross, N. Galili, *Angew. Chem. Int. Ed.* **1999**, *38*, 2366 – 2369; *Angew. Chem.* **1999**, *111*, 2536 – 2540; c) L. Simkhovich, P. Iyer, I. Goldberg, Z. Gross, *Chem. Eur. J.* **2002**, *8*, 2595 – 2601.

[21] a) P. Jiang, Z. Guo, *Coord. Chem. Rev.* **2004**, *248*, 205 – 229; b) K. P. Carter, A. M. Young, A. E. Palmer, *Chem. Rev.* **2014**, *114*, 4564 – 4601.

Received: September 21, 2015
Revised: November 5, 2015
Published online: December 2, 2015

